TROPICAL WESTERN PACIFIC THERMAL STRUCTURE AND ITS RELATIONSHIP TO OCEAN SURFACE VARIABLES

A NUMERICAL STATE ESTIMATE AND FOREREEF TEMPERATURE RECORDS

By Travis A. Schramek,
Bruce D. Cornuelle,
Ganesh Gopalakrishnan,
Patrick L. Colin,
Sonia J. Rowley,
Mark A. Merrifield,
and Eric J. Terrill

ABSTRACT. Complex interactions between open ocean and nearshore environments pose a predictability problem. Basin-scale ocean models are typically run at grid scales that do not accurately resolve individual islands, and model output is assessed mostly using observations of the open ocean. Thus, model ability to replicate island forereef oceanic variability has gone largely untested. Here, an eight-year regional state estimate covering 2009–2017 is compared to bottom temperature observations at the western Pacific islands of Palau and Pohnpei, and is found to reproduce the observed seasonal to interannual variability. Because of their steep bathymetry, these islands can act as moorings. Sea surface variables, such as temperature (SST) and height (SSH), have been shown to predict upper ocean thermal structure in the region, but the spatial structure of the relationship has gone unexplored. The state estimate was used to examine the multivariate predictability of temperature at depths to about 200 m both at the island boundaries and throughout the domain. The results show that the best multiple linear regression (MLR) skill was found near Palau, but useful skill (>0.6) was available through much of the region within the anticyclonic gyre driven by positive wind-stress curl. Point SSH measurements offered prediction skill for areas extending a few hundred kilometers zonally and perhaps 100 km meridionally. The insights into the additional information contained in surface variables in this region could aid in advancement of ocean modeling as well as predictions of ecological patterns and stressors.

ABOVE. Looking down from 90 m below the ocean's surface, Patrick Colin captured fellow scientific diver Steve Lindfield ascending up a reef wall in Palau. The pair of divers were on a mission to recover temperature gauges deployed the prior year and photograph mesophotic coral ecosystems. These temperature data are leveraged in this manuscript to assess the full physics circulation model run for the tropical western Pacific. *Photo Credit: Patrick L. Colin, CRRF*

IN PLAIN WORDS. Predicting how waters directly on an island forereef change over time is a complex problem. Even with twenty-first century computing techniques, large efforts are required to model and forecast changes in subsurface temperature. We test how one of these ocean models performs using observations of ocean temperature collected by diver-deployed instruments placed on the forereefs of both Palau and Pohnpei. We show that these models do well at matching the temperature changes seen by the diver-deployed instruments between 2009 and 2017. Additionally, the link between sea level and subsurface temperature changes is shown to be strong around Palau and throughout the Caroline Islands. These advances can help predict coral bleaching events and the locations of vessels that might be fishing in the region.

INTRODUCTION

The near-island oceanographic environment contains dynamics that span submeso- to basin scales. This range in spatial and associated temporal scales poses a predictability problem around island groups. Computation and storage costs generally limit the resolution of operational models that require nesting from open ocean conditions down to scales that resolve forereefs of O(10–100) m. However, insights gleaned from sustained observations collected over decades from bottom-mounted sensors installed around islands may contribute to solving this prediction problem. These sensors, aimed at studying nearshore and regional phenomena (Roemmich, 1984; Gove et al., 2015; Williams et al., 2018), also captured the large spatial scale dynamics and seasonal to interannual variability that these models best address.

Here, we attempt to better understand ocean-island interactions as a part of the Office of Naval Research (ONR) Flow Encountering Abrupt Topography (FLEAT) Departmental Research Initiative (DRI). FLEAT aims to bridge the scales that extend from operational modeling of the global ocean to regional flow fields that run into topography, such as island groups. Ocean state estimates, like operational global models, permit contextualization of observational records and their physical drivers but can lack fully resolved bathymetry due to operational constraints. The state estimates used here are based on the Massachusetts Institute of Technology general circulation model (MITgcm; Adcroft et al., 1997; Marshall et al., 1997)

and Estimating the Circulation and Climate of the Ocean (ECCO; Stammer et al., 2002) four-dimensional variational assimilation (4DVAR) system and are denoted as the Western Pacific Ocean State Estimate (WPOSE). The WPOSE domain is 115°E–170°E, 15°S–27°N. The state estimate supplies a continuous, fully resolved set of model fields for comparison to observations and, in this case, for estimating relationships between different ocean variables, and so generalize the results from the point observations and put them into context.

As a part of the FLEAT ONR DRI, analysis was done on oceanographic observations from both Palau (7.5°N, 134.5°E) and the island of Pohnpei (8.0°N, 158.2°E), both of which are in the tropical northwestern Pacific (**Figure 1**). Palau, an independent nation, sits roughly 2,600 km west of Pohnpei, which is a part of the Federated States of Micronesia. Similar oceanographic conditions exist at both sites, with the North Equatorial Current (NEC) flowing westward north of them and the North Equatorial Countercurrent (NECC) flowing eastward at their latitude band or just south of them (Heron et al., 2006; Hsin and Qiu, 2012; Chen et al., 2016). Observational studies show interannual and seasonal variability in the flow field and upper ocean structure near Palau (Heron et al., 2006; Schramek et al., 2018), as well as active internal wave fields (Wolanski et al., 2004; Colin, 2018; Rowley et al., 2019).

Variability in the depth of the thermocline in this region drives changes in both nearshore and open ocean biological communities such as coral reef

ecosystems and pelagic fisheries. Cold waters transported vertically by thermocline displacements can supply nutrients to the shallow coral reef ecosystems. Variations in upwelling on reef slopes in the tropical Pacific can dictate coral feeding habits and survival during stress events (M.D. Fox et al., 2018; Williams et al., 2018). Farther offshore, sea surface height (SSH) as well as other proxies for thermocline depth have been shown to have predictability in relating ocean variability to the locations of fishing vessels (Cimino et al., 2019). Better predictability of thermocline displacements in the tropical Pacific and around islands could help inform the biological oceanography community on these emerging problems in ecosystem health.

In this region, the vertical structure of ocean properties in the open ocean has been shown to be predictable using real-time satellite observations. SSH in the tropical Pacific Ocean acts as an indicator for thermocline depth (Rebert et al., 1985) as well as for the depth of the 20°C isotherm (Chaen and Wyrtki, 1981). This concept, coupled with altimetry products, has led to the generation of synthetic temperature profiles (Carnes et al., 1990) and has been used to aid typhoon intensity forecasts (Pun et al., 2007). Ocean state estimates also use SSH to infer subsurface displacement fields where subsurface data are sparse (D.N. Fox et al., 2002). This relationship exists in the region because there is strong stratification and dominance of baroclinic variability in this meridional band. Subsurface ocean temperatures directly adjacent to island boundaries, specifically at Palau, have been shown to be predictable from satellite-derived SSH and sea surface temperature (SST; Schramek et al., 2018). While this recent extension of the understanding of the relevance of open ocean processes to forereef environments was shown observationally in one location, it was not possible to assess the utility of the method in a spatially discretized sense. Pun et al. (2007) showed meridional differences in the efficacy of

predicting upper ocean thermal structure using surface variables, but with averages taken over large latitude bands. WPOSE provides a means for assessing the spatial differences in skill, adding in the zonal component.

This article addresses the following hypotheses: (1) WPOSE can reproduce observed nearshore temperature variability, including the relationships between SST, SSH, and subsurface temperature; (2) WPOSE SSH and SST can be used to estimate subsurface temperature over much of the region; and (3) horizontal correlation scales of SSH signals and thermocline depths allow SSH at a point, such as a tide gauge, to be an indicator of time-varying thermocline displacement within a 100–200 km range.

To test these hypotheses, we first assess WPOSE output in relation to in situ observations of temperature collected by bottom-mounted thermographs that extend to maximum depths of 90 m and 130 m at Palau and Pohnpei, respectively. Next, we assess the relationship between SST and SSH and subsurface temperatures. Predictability of subsurface temperatures using SST and SSH is tested over a subset of the WPOSE domain, including Palau and Pohnpei. We test the zonal and meridional extent of the region within which point measurements of SST and SSH can be used as predictors of subsurface variability, both at specified depths and at thermocline depths, which vary spatially.

MODEL, DATA, AND METHODS

We use the WPOSE solutions for the period of January 2009 to December 2017. WPOSE is a regional implementation of the MITgcm, simulated in hydrostatic mode, with the adjoint-based ECCO 4DVAR assimilation system. It uses a four-month non-overlapping assimilation window, meaning that the model controls, including temperature and salinity initial conditions, open-ocean boundary conditions, and atmospheric forcings, are adjusted every four months, providing free simulations forced using adjusted controls during each window. The state estimate was analyzed in studies of the circulation of the tropical western Pacific (Lien et al., 2015; Qiu et al., 2015; Schönau et al., 2015). The state estimates are constrained to fit observations within the region 122°E–170°E and 5°N–20°N, including satellite-derived SSH and SST, Argo and XBT profiles, Spray glider missions, and mooring deployments. Both the initial (first) guess and the final (optimized) solution for the estimates are assessed to determine their fit with observations.

The state estimates are available on a 1/6° grid, but the solutions are smooth and there is little structure at the smallest scales. The state estimates obey the model dynamics but should be close enough to the real ocean evolution to be compared directly, not just statistically. Model controls, including temperature and salinity initial conditions, open-ocean boundary conditions, and atmospheric forcings are adjusted in WPOSE to minimize a "cost function" defined by the weighted sum of quadratic norms of both model-data misfit and changes to control variables between the initial time and the final time of the assimilation period (four months). The adjustments are made using a numerically generated gradient (adjoint) using the Transformations of Algorithms in Fortran (Giering and Kaminski, 1998; Heimbach et al., 2002) of the ocean model that calculates how the cost function can be reduced by making changes to the model controls. In this case, the initial estimate (first guess), which comes from the real-time US Navy HYCOM/NCODA 1/12 global analysis (https://www.hycom.org/dataserver/gofs-3pt1/analysis; Chassignet et al., 2007), is already very good, and the iterative optimization reduces the cost function by about half on average. The mini-
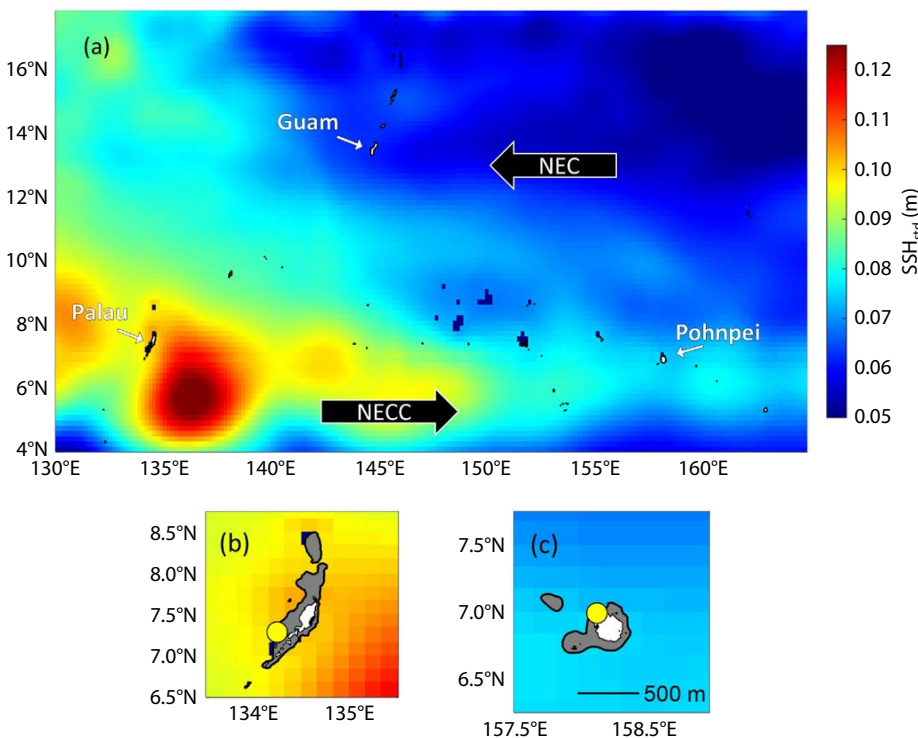

FIGURE 1. (a) The standard deviation of sea surface height (SSH) across a subset of the Western Pacific Ocean State Estimate (WPOSE) domain within the tropical northwestern Pacific is computed here over the full run of WPOSE between January 2009 and December 2017. The islands of Palau, Pohnpei, and Guam are labeled. All islands within the displayed model domain are shown in white with a black boarder. (b) The yellow dot marks the location of the bottom-mounted temperature array at Ulong Rock on Palau. (c) The yellow dot denotes the Pohnpei observation station (Obs) at Palikir reef. In (b) and (c), the 500 m bathymetric contour is shown in black and the gray shading denotes areas shallower than 500 m depth.

mization of the cost function takes place iteratively. At each iteration, the misfit between the model and the observations is calculated for the latest simulation. The adjoint is calculated as a linearization around the current guess and produces the gradient of the cost function with respect to the controls, which is used to generate a new solution using iterative optimization via a variable-storage Quasi-Newton M1NQ3 algorithm (Gilbert and Lemaréchal, 1989). The estimates used here are available at http://ecco.ucsd.edu/nwpac_results1.html.

Temperature observations were made in the waters of the western Pacific island nation of Palau, where the main island group sits at 7.5°N, 134.5°E (Figure 1a). An array of bottom-mounted thermograph stations was established by the Coral Reef Research Foundation in January 2000 and was still being maintained at the time of this publication. Observations made between January 2009 and May 2016 are used in this study. Stations at Ulong Rock on the southwest forereefs of Palau (yellow dot in Figure 1b) were occupied in depths ranging between 2 m and 90 m. Sampling rates varied between 1 minute and 30 minutes over the course of the records. Analysis in this manuscript is done on daily averages of the observations. A detailed description of the observational array can be found in the methods and supplemental materials of Schramek et al. (2018).

Observations of bottom temperature were also made on the forereef of the island of Pohnpei, located in the Federated States of Micronesia (FSM) at approximately 8.0°N, 158.2°E (Figure 1a). Stations were maintained under a University of Hawai'i at Mānoa research program between August 2015 and July 2016. Depths of 10 m to 130 m were occupied as a part of a study of mesophotic coral reef ecosystems in the FSM. Sampling was done at 30-minute intervals across the array.

Multiple linear regression (MLR; Chatterjee and Hadi, 1986) was used on the state estimates to assess the capabil-

ity of reconstructing subsurface temperatures with ocean surface variables SSH and SST. Regressions were computed independently for each depth level using the local SST and SSH as predictors in the MLR, and later using SSH and SST only at Palau or Pohnpei to estimate temperature through MLR across the domain and all depths above 200 m.

RESULTS
WPOSE Assessment
SSH standard deviation for a subset of the WPOSE domain (Figure 1a) shows elevated standard deviations of SSH in the latitude band between 5°N and 8°N, at the interface between the NEC and NECC. Structure in the SSH variability near Palau results from standing eddies of the NECC, which have high spatial variability (Figure 1a). The zonal peak in SSH variability is within the footprint of the seasonal Caroline Eddy (Heron et al., 2006), located southeast of Palau. The magnitude of the SSH variability provides a means of assessing whether the thermocline displacement can have an observable surface signature.

The upper ocean temperature structure and variability captured by the bottom-mounted thermograph observa-

tions at Palau were compared to a model grid point nearest to the measurement. The chosen model grid points were in deep water because the steep topography of Palau goes from land to deep water in a single grid point. Although these observations spanned the eight-year duration of the state estimate, they were not used in the state estimate. Mean temperature profiles observed at Palau between 2 m and 90 m depth are similar to the state estimate (Figure 2a). The seasonal and interannual variability, such as that associated with the El Niño-Southern Oscillation (ENSO), dominates the correlation computed between the observations and the model output (Figure 2b). Differences between the initial run of WPOSE and the final state do not show large differences on interannual timescales, suggesting that the first-guess solution initialized from HYCOM/NCODA analysis captures the same variability. Correlations from the optimized state range from 0.80–0.91 and shows slight improvements over the first-guess solution.

Intraseasonal and high-frequency variabilities in the temperature observations are likely driven by mesoscale and submesoscale dynamics such as coastally trapped waves, internal wave fields, and
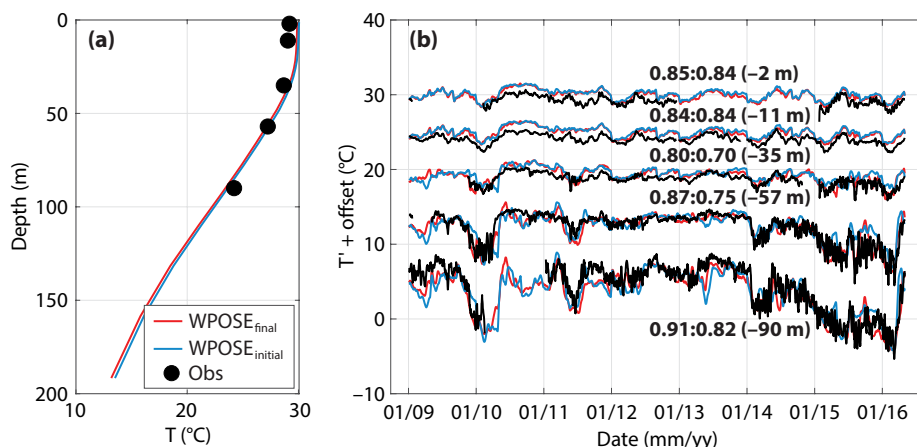

FIGURE 2. (a) Mean temperature profile at Palau in the upper 200 m between January 2009 and May 2016 as observed by bottom-mounted thermographs (black dots) and compared to model output from WPOSE (red line) and the initial state guess in WPOSE (blue line). This is a subset of the temperature observations within the state estimate time range. (b) Daily averaged temperature records from each depth station are shown (black lines) with the depths noted in text. The y-axis is temperature, with temperature at deeper depth levels sequentially offset by −5°C. Reference temperatures are marked from 40°C to −10°C. The values written above the curves are the correlation coefficients for Observations vs WPOSE$_{final}$:Observations vs WPOSE$_{initial}$ and corresponding depth levels appear in parentheses.

eddies, which have been shown to be present in the region (Wolanski et al., 2003, 2004; Colin, 2009, 2018). These dynamics can be present in the model but are not expected to be realistically represented in relation to the in situ records. WPOSE is not forced using tide or atmospheric pressure forcing and is not designed to resolve the phase of internal wave fields around the island. Also, the model bathymetry is not optimized to represent topographic wave variability around the islands.

One year of bottom temperature observations from the forereefs of Pohnpei between 10 m and 130 m depth were compared to WPOSE temperatures at the closest grid point and depth levels (Figure 3a). Again, these observations were not used in the estimate. Correlations for the state estimate range between 0.62 and 0.93, with the maximum centered on the depth range of 60 m to 130 m (Figure 3b) and lower correlations at 40 m depth and above. In this case, the first guess outperformed the state estimate below 40 m. The temperature observations for this single year were made between 2015 and 2016, the period when the El Niño event decayed. A large suppression of the thermocline was first observed at Pohnpei starting in January 2016 (Figure 3b), and was later observed at Palau starting in March 2016 (Figure 2b). This is hypothesized to be a Rossby wave-like structure that propagated westward across the tropical Pacific. The relatively short record leads to less weight on the seasonal to interannual variability that is of most interest. The first guess for WPOSE closely resembles HYCOM/NCODA for the area due to its initialization and performs better than the optimized solution. We hypothesize that this is because observations were only assimilated within the region of 122°E–170°E and 5°N–20°N; Pohnpei is at the southeastern edge of the domain, so it does not benefit as much from the assimilations at Palau, which preform better than future WPOSE runs.

In addition, while satellite SSH and SST cover the whole region, in situ observations are concentrated near Palau. This suggests that WPOSE is less constrained near Pohnpei than Palau, and the remoteness of Pohnpei from the majority of the assimilated in situ observations might have caused the increase in differences seen over the one-year temperature comparison. However, for the analysis of the MLR performance, the differences are small, and the exploration of the relationship between SST, SSH, and subsurface temperature can be done in either the first guess or the state estimate.

The depth structure of ocean temperatures in this subdomain are dominated by the effects of the positive wind stress curl-driven gyre that includes part of the NEC to the north and the NECC to the south. The depth of the maximum in the vertical derivative of potential temperature, dT/dz, denoted henceforth as thermocline depth, at each grid cell reflects the zonal structure set up by this atmospheric forcing (Figure 4). This is the signature of the NEC to the north and the NECC to the south of the latitude band of both Palau and Pohnpei. The semi-persistent meander of the NECC southwest of Palau (Figure 4) can be seen in the temperature field to the south of Palau (not shown).
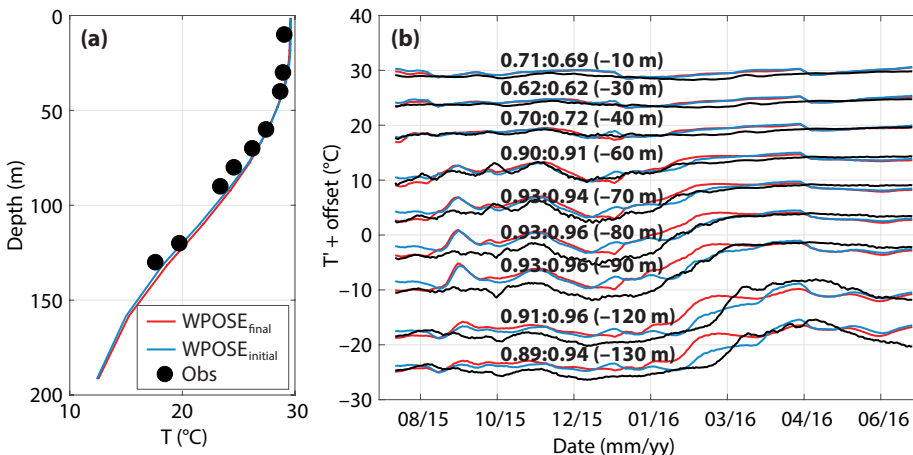
Sea Surface Height and Subsurface Temperatures

SSH is related to the temperature at the thermocline depth across the tropical northwestern Pacific. MLRs were com-

FIGURE 3. (a) Mean temperature profile at Pohnpei in the upper 200 m between August 2015 and July 2016 as observed by bottom-mounted thermographs (black dots), with the state estimate (red line) and the initial state guess (blue line) plotted. (b) Daily averaged temperature records from each depth station (black line) with depths noted in text. The y-axis is temperature, with temperature at each depth level sequentially offset by −5°C. Reference temperatures are marked from 40°C to −30°C. The values labeled above each curve are the correlation coefficients for Observations vs WPOSE$_{final}$:Observations vs WPOSE$_{initial}$ and corresponding depth levels appear in parentheses.
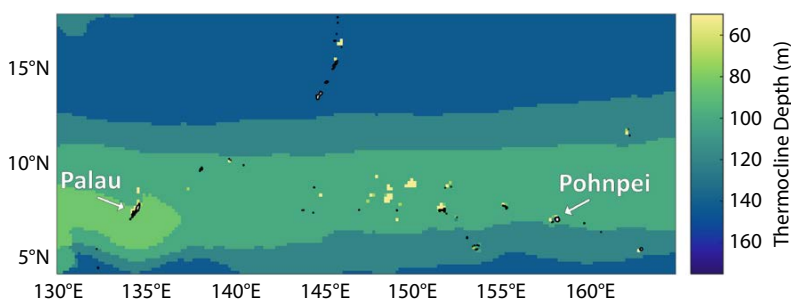

FIGURE 4. The thermocline depth, determined here as the depth of the maximum in dT/dz, which can be considered the midpoint of the thermocline, is shown for the tropical northwestern Pacific. This is computed as a mean over the entire run of WPOSE. The model grid depth level discretization has not been smoothed.

puted at each WPOSE grid point using the local SSH, SST, and T(z). Skill values of at least 0.7 were seen across the domain in the latitude band of 6°N to 10°N (Figure 5a). Maxima of the skill were evident southeast of Palau and in its immediate vicinity. Depth profiles of the fraction of variance explained, also noted as the skill, by SSH, SST, and the MLR, showed similar results between Palau (Figure 5b) and Pohnpei (Figure 5c). The MLR performed nearly perfectly at the surface at both locations, as SST was being used as an input to the MLR. MLR skill decreases with depth, with a minimum at the depth where SST's and SSH's roles as ocean surface proxies for subsurface temperature cross over (Figure 5b,c). This is the depth zone where the multivariate property of the MLR is clearest, because significant skill reduction would occur if either variable were used alone to estimate T(z). SSH continues to be a predictor of T(z) through the depth of the thermocline shown in Figure 4a. The depth structure of the MLR skill at Palau compares well to the results found using observed SSH at Palau in the Supplemental Figure S4b of Schramek et al. (2018). These results are consistent with Pun et al. (2007) in the meridional region of overlap between the studies, 9°N–17°N.

The relationship between SSH and temperature in the thermocline has a horizontal decay scale of O(100) km. SSH and SST at Palau were used as the predictors for MLR across the domain, predicting subsurface temperatures at all grid points (Figure 6a). WPOSE allows for this detailed spatial analysis, which otherwise is not possible in the absence of sustained and spatially dense observations within the domain. This MLR was done to determine the spatial scales of SSH's influence near the Palau main island group. Useful skill extends upward of 200 km to the east of the island group. A weaker relationship between SSH at Palau and T(92 m) is found across the domain centered on the 6°N to 10°N latitude band. T(92 m) is used for this analysis as it is a depth level that is consistently within the thermocline. The same test was done using SST and SSH at Pohnpei (Figure 6b). The skill around Pohnpei is lower than was found around Palau but falls off less rapidly to the east and west.

The skill of MLRs reproducing temperatures at the mean depths of the thermocline (Figure 7) shows a maximum in the latitude band of Palau and Pohnpei. Skill fades to the north and south. This zonal band of maximum skill is hypothesized to reflect the positive wind curl raising and sharpening the thermocline, allowing the MLR to work well. The persistent meander of the NECC to the south of Palau is also evident in this result. The discrete vertical grid in WPOSE pro-
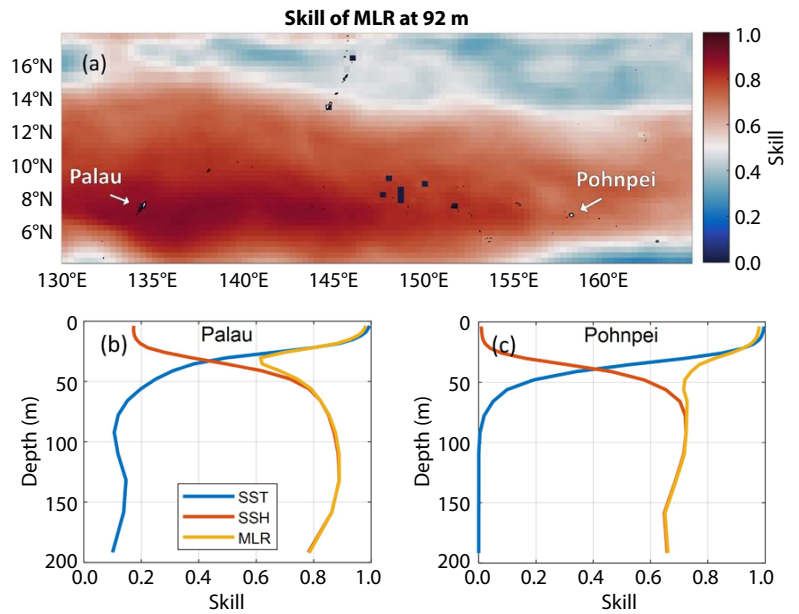

FIGURE 5. (a) Regional plot of the skill of the multiple linear regression (MLR) at 90 m. For (b) Palau and (c) Pohnpei, depth profiles of the fraction of variance explained by the MLR (yellow) as well as SST (blue) and SSH (orange) are plotted individually.
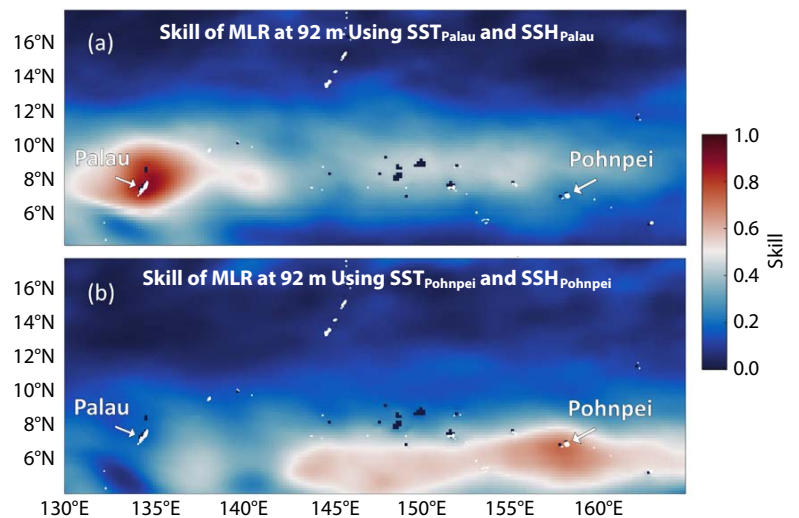

FIGURE 6. The MLR skill when using SST and SSH from a single point at (a) Palau and (b) Pohnpei as the predictor in MLRs at all locations to predict the temperature at 92 m across the domain.
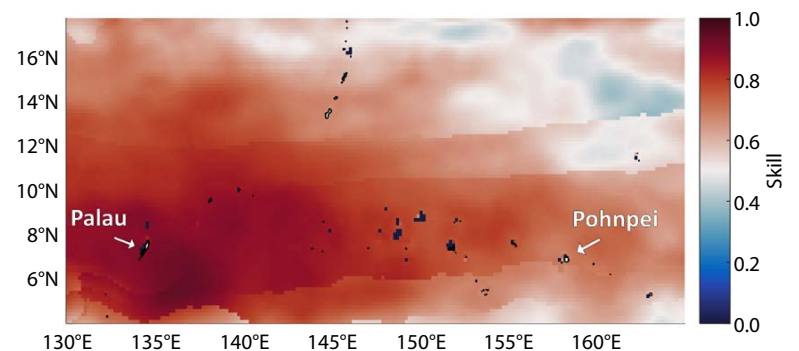

FIGURE 7. The skill of the MLR at the thermocline depth for each respective grid point is shown. Any red color on a grid cell indicates skill of at least 0.5 based on the colormap.

duces zonal banding in the depth of the mixed layer and the subsequent banding present in Figure 7.

DISCUSSION
We found that the state estimate, and even the first guess before optimization, captured the upper ocean temperature structure in the mean and seasonal to interannual variability as observed at Palau and Pohnpei (Figures 1 and 2). The relation between SST, SSH, and temperature is also similar to observations. Sustained observations at Palau to depths of 90 m showed correlations up to 0.91 with WPOSE solutions (Figure 2b). Comparisons of observation at Pohnpei made over 2015–2016 gave insight into the ability of the model to recreate the ocean state across the domain (Figure 3), specifically for the decay of the 2015–2016 El Niño event. WPOSE is best suited for reproducing seasonal to interannual variability. Additional and longer-term observations and a model and assimilation system more centered on Pohnpei would be useful for better testing of the state estimation at this location. Additional validation of WPOSE is contained in Schönau et al. (2019) in this special issue of *Oceanography*.

The state estimate provided a physically constrained complete data set to assess how well SST and SSH could estimate subsurface temperature structure across the tropical northwestern Pacific. MLRs were computed at all locations (Figure 5a) and also from two individual grid points (Figure 6a,b), mimicking the use of an SSH and SST gauge station, surface mooring, or repeat satellite observation point to drive an MLR across the region. MLRs computed at Palau and Pohnpei were consistent with previous results found using in situ SSH and remotely sensed SST (Figure 5; Schramek et al., 2018). The fraction of variance explained (skill) by SST was shown to decrease with depth from ~1 at the surface at both locations, while the skill of SSH increased with depth (Figure 5b,c). Across the region, MLR skill in predict-

ing T(92 m), a depth level consistently near the thermocline, was highest in the zonal band between 6°N and 10°N. Elevated standard deviation of SSH in the region (Figure 1a) corresponds well with the skill of local SSH predicting local subsurface temperatures (Figure 5a).

The ability to use SSH from a single grid point, mimicking the use of a single in situ station—a reality of spatially sparse observations—to predict T(z) via MLR across the domain was also assessed (Figure 6). SSH at Palau can predict T(92 m) with skill >0.9, within 1°–2° of latitude or longitude around the main island group of Palau (Figure 6a). This corresponds well with the large amount of variability in SSH near Palau (Figure 1a,b). In contrast, the skill of SSH in predicting T(92 m) is lower at Pohnpei where SSH variability is smaller (Figure 1a). Skill does remain >0.7 in the upper 100 m of the water column (Figure 5c), showing SSH is still a good indicator of subsurface variability at that location.

Finally, SSH was assessed as an indicator of temperature at the mean depth of the thermocline at each grid point (Figure 7). This provides a maximum estimate of skill when predicting at discrete depths. MLR skill in predicting temperature at the mean depth of the thermocline largely matches that of the standard deviation of SSH (Figures 1 and 7), although with some areas of exception. This fits with the hypothesis that SSH acts as an indicator of variability at the thermocline in the region.

The MLR uses both SST and SSH in the prediction of T(z) within the depth transition between the upper mixed layer and the thermocline. This multivariate property extends the literature, which mainly assesses SSH in predicting T(z) (Chaen and Wyrtki, 1981; Rebert et al., 1985), and supports Pun et al. (2007) in formulating an operational concept for predicting upper ocean temperature structure from the surface down through the thermocline using multiple ocean surface variables, now with assessments of spatial skill.

Isotherm displacement can more easily be calculated from the model than from the observations and is better suited to this style of analysis. Chaen and Wyrtki (1981) showed that SSH related well to isotherm displacement. This analysis could be reproduced to track isotherms, and we hypothesize that it could provide similar or better skills than those discussed here. Work in displacement modes has shown that this is a less noisy predictor for variability in isotherm depth. Issues with nonlinearity in temperature regressions would also be eliminated.

Predicting subsurface temperatures from ocean surface variables contributes to a range of operational oceanographic and ecological problems. Coral bleaching is assessed and predicted by using SST to calculate cumulative anomalous heat at a certain location (Strong et al., 2004). Utilizing the predictive capabilities shown here and in previous work, managers and researchers of coral reef ecosystems can better predict temperature anomalies at depths from the surface to into the mesophotic zone (30–150 m) in this region. Enhancing predictability can aid in the direction of pre- and post-bleaching event surveys aimed toward better understanding of the role of oceanographic structure on coral ecosystem health. Additionally, thermocline depth and sea surface height have been shown to be predictors of where successful fishing for pelagic species occurs in Palau's Economic Exclusion Zone (Cimino et al., 2019). This analysis has helped better explain the spatial structure of the expected skill of those variables, which can contribute to the development of future fisheries enforcement techniques.

REFERENCES
Adcroft, A., C. Hill, and J. Marshall. 1997. Representation of topography by shaved cells in a height coordinate ocean model. *Monthly Weather Review* 125(9):2,293–2,315, https://doi.org/10.1175/1520-0493(1997)125<2293:ROTBSC>2.0.CO;2.
Carnes, M.R., J.M. Mitchell, and P.W. deWitt. 1990. Synthetic temperature profiles derived from Geosat altimetry: Comparison with air-dropped expendable bathythermograph profiles. *Journal of Geophysical Research* 95(C10):17,979–17,992, https://doi.org/10.1029/JC095iC10p17979.

Chaen, M., and K. Wyrtki. 1981. The 20°C isotherm depth and sea level in the western equatorial pacific. *Journal of the Oceanographical Society of Japan* 37(4):198–200, https://doi.org/10.1007/BF02309057.

Chassignet, E.P., H.E. Hurlburt, O.M. Smedstad, G.R. Halliwell, P.J. Hogan, A.J. Wallcraft, R. Baraille, and R. Bleck. 2007. The HYCOM (HYbrid Coordinate Ocean Model) data assimilative system. *Journal of Marine Systems* 65(1):60–83, https://doi.org/10.1016/j.jmarsys.2005.09.016.

Chatterjee, S., and A.S. Hadi. 1986. Influential observations, high leverage points, and outliers in linear regression. *Statistical Science* 1(3):379–393.

Chen, X., B. Qiu, Y. Du, S. Chen, and Y. Qi. 2016. Interannual and interdecadal variability of the North Equatorial Countercurrent in the western Pacific. *Journal of Geophysical Research* 121(10):7,743–7,758, https://doi.org/10.1002/2016JC012190.

Cimino, M.A., M. Anderson, T. Schramek, S. Merrifield, and E.J. Terrill. 2019. Towards a fishing pressure prediction system for a western Pacific EEZ. *Scientific Reports* 9(1):461, https://doi.org/10.1038/s41598-018-36915-x.

Colin, P.L. 2009. *Marine Environments of Palau*. Indo-Pacific Press, Taiwan, http://coralreefpalau.org/wp-content/uploads/2017/04/Colin-PL-2009-Marine-Environments-of-Palau.pdf.

Colin, P.L. 2018. Ocean warming and the reefs of Palau. *Oceanography* 31(2):126–135, https://doi.org/10.5670/oceanog.2018.214.

Fox, D.N., W.J. Teague, C.N. Barron, M.R. Carnes, and C.M. Lee. 2002. The Modular Ocean Data Assimilation System (MODAS). *Journal of Atmospheric and Oceanic Technology* 19(2):240–252, https://doi.org/10.1175/1520-0426(2002)019<0240:TMODAS>2.0.CO;2.

Fox, M.D., G.J. Williams, M.D. Johnson, V.Z. Radice, B.J. Zgliczynski, E.L.A. Kelly, F.L. Rohwer, S.A. Sandin, and J.E. Smith. 2018. Gradients in primary production predict trophic strategies of mixotrophic corals across spatial scales. *Current Biology* 28(21):3,355–3,363.E4, https://doi.org/10.1016/j.cub.2018.08.057.

Giering, R., and T. Kaminski. 1998. Recipes for adjoint code construction. *ACM Transactions on Mathematical Software* 24(4):437–474, https://doi.org/10.1145/293686.293695.

Gilbert, J.C., and C. Lemaréchal. 1989. Some numerical experiments with variable-storage quasi-Newton algorithms. *Mathematical Programming* 45(1):407–435, https://doi.org/10.1007/BF01589113.

Gove, J.M., M.A. McManus, A.B. Neuheimer, J.J. Polovina, J.C. Drazen, C.R. Smith, M.A. Merrifield, A.M. Friedlander, J.S. Ehses, C.W. Young, and others. 2015. Near-island biological hotspots in barren ocean basins. *Nature Communications* 7:10581, https://doi.org/10.1038/ncomms10581.

Heimbach, P., C. Hill, and R. Giering. 2002. Automatic generation of efficient adjoint code for a parallel Navier-Stokes solver. Pp. 1,019–1,028 in *Computational Science — ICCS 2002*. P.M.A. Sloot, A.G. Hoekstra, C.J.K. Tan, and J.J. Dongarra, eds, Springer, Berlin Heidelberg.

Heron, S.F., E.J. Metzger, and W.J. Skirving. 2006. Seasonal variations of the ocean surface circulation in the vicinity of Palau. *Journal of Oceanography* 62(1992):413–426, https://doi.org/10.1007/s10872-006-0065-3.

Hsin, Y.C., and B. Qiu. 2012. Seasonal fluctuations of the surface North Equatorial Countercurrent (NECC) across the Pacific basin. *Journal of Geophysical Research* 117(6), https://doi.org/10.1029/2011JC007794.

Lien, R.-C., B. Ma, C. Lee, T. Sanford, V. Mensah, L. Centurioni, B.D. Cornuelle, G. Gopalakrishnan, A.L. Gordon, M.-H. Chang, and others. 2015. The Kuroshio and Luzon Undercurrent east of Luzon Island. *Oceanography* 28(4):54–63, https://doi.org/10.5670/oceanog.2015.81.

Marshall, J., A. Adcroft, C. Hill, L. Perelman, and C. Heisey. 1997. A finite-volume, incompressible Navier Stokes model for studies of the ocean on parallel computers. *Journal of Geophysical Research* 102(C3):5,753–5,766, https://doi.org/10.1029/96JC02775.

Pun, I., I. Lin, C. Wu, D. Ko, and W.T. Liu. 2007. Validation and application of altimetry-derived upper ocean thermal structure in the western North Pacific Ocean for typhoon-intensity forecast. *IEEE Transactions on Geoscience and Remote Sensing* 45(6):1,616–1,630, https://doi.org/10.1109/TGRS.2007.895950.

Qiu, B., D. Rudnick, I. Cerovecki, B. Cornuelle, S. Chen, M. Schönau, J.L. McClean, and G. Gopalakrishnan. 2015. The Pacific North Equatorial Current: New insights from the origins of the Kuroshio and Mindanao Currents (OKMC) Project. *Oceanography* 28(4):24–33, https://doi.org/10.5670/oceanog.2015.78.

Rebert, J.P., J.R. Donguy, G. Eldin, and K. Wyrtki. 1985. Relations between sea level, thermocline depth, heat content, and dynamic height in the tropical Pacific Ocean. *Journal of Geophysical Research* 90(C6):11,719–11,725, https://doi.org/10.1029/JC090iC06p11719.

Roemmich, D. 1984. Indirect sensing of equatorial currents by means of island pressure measurements. *Journal of Physical Oceanography* 14(9):1,458–1,469, https://doi.org/10.1175/1520-0485(1984)014<1458:ISOECB>2.0.CO;2.

Rowley, S.J., T.E. Roberts, R.R. Coleman, H.L. Spalding, E. Joseph, and M.K.L. Dorricott. 2019. Pohnpei, Federated States of Micronesia. Pp. 301–320 in *Mesophotic Coral Ecosystems*. Y. Loya, K.A. Puglise, and T.C.L. Bridge, eds, Coral Reefs of the World, vol. 12, Springer, Cham, https://doi.org/10.1007/978-3-319-92735-0_17.

Schönau, M., D. Rudnick, I. Cerovecki, G. Gopalakrishnan, B. Cornuelle, J. McClean, and B. Qiu. 2015. The Mindanao Current: Mean structure and connectivity. *Oceanography* 28(4):34–45, https://doi.org/10.5670/oceanog.2015.79.

Schönau, M.C., H.W. Wijesekera, W.J. Teague, P.L. Colin, G. Gopalakrishnan, D.L. Rudnick, B.D. Cornuelle, Z.R. Hallock, and D.W. Wang. 2019. The end of an El Niño: A view from Palau. *Oceanography* 32(4):32–45, https://doi.org/10.5670/oceanog.2019.409.

Schramek, T.A., P.L. Colin, M.A. Merrifield, and E.J. Terrill. 2018. Depth-dependent thermal stress around corals in the tropical Pacific Ocean. *Geophysical Research Letters* 45(18):9,739–9,747, https://doi.org/10.1029/2018GL078782.

Smith, W.H., and D.T. Sandwell. 1997. Global sea floor topography from satellite altimetry and ship depth soundings. *Science* 277(5334):1,956–1,962, https://doi.org/10.1126/science.277.5334.1956.

Stammer, D., C. Wunsch, R. Giering, C. Eckert, P. Heimbach, J. Marotzke, A. Adcroft, C.N. Hill, and J. Marshall. 2002. Global ocean circulation during 1992–1997, estimated from ocean observations and a general circulation model. *Journal of Geophysical Research* 107(C9):1-1–1-27, https://doi.org/10.1029/2001JC000888.

Strong, A.E., G. Liu, J. Meyer, J.C. Hendee, and D. Sasko. 2004. Coral reef watch 2002. *Bulletin of Marine Science* 75(2):259–268.

Williams, G.J., S.A. Sandin, B.J. Zgliczynski, M.D. Fox, J.M. Gove, J.S. Rogers, K.A. Furby, A.C. Hartmann, Z.R. Caldwell, N.N. Price, and J.E. Smith. 2018. Biophysical drivers of coral trophic depth zonation. *Marine Biology* 165:60, https://doi.org/10.1007/s00227-018-3314-2.

Wolanski, E., R.H. Richmond, G. Davis, E. Deleersnijder, and R.R. Leben. 2003. Eddies around Guam, an island in the Mariana Islands group. *Continental Shelf Research* 23(10):991–1,003, https://doi.org/10.1016/S0278-4343(03)00087-6.

Wolanski, E., P. Colin, J. Naithani, E. Deleersnijder, and Y. Golbuu. 2004. Large amplitude, leaky, island-generated, internal waves around Palau, Micronesia. *Estuarine, Coastal and Shelf Science* 60(4):705–716, https://doi.org/10.1016/j.ecss.2004.03.009.

AUTHORS
Travis A. Schramek (tschramek@ucsd.edu) is an oceanographer, **Bruce D. Cornuelle** is Research Oceanographer, and **Ganesh Gopalakrishnan** is Project Scientist, all at Scripps Institution of Oceanography, University of California San Diego, La Jolla, CA, USA. **Patrick L. Colin** is Director, Coral Reef Research Foundation, Koror, Palau. **Sonia J. Rowley** is Postdoctoral Researcher, University of Hawai'i at Mānoa, Honolulu, HI, USA. **Mark A. Merrifield** is Professor, Scripps Institution of Oceanography, University of California San Diego, La Jolla, CA, USA. **Eric J. Terrill** is Director, Coastal Observing Research and Development Center, Scripps Institution of Oceanography, University of California San Diego, La Jolla, CA, USA.